radiation

MDPI

Article

Risk Assessment of Exposure to Natural Radiation in Soil Using RESRAD-ONSITE and RESRAD-BIOTA in the Cobalt-Nickel Bearing Areas of Lomié in Eastern Cameroon

Gondji Dieu Souffit [1,2], Saïdou [1,2,*], Oumar Bobbo Modibo [2,3], David Lepoire [4] and Shinji Tokonami [3]

[1] Nuclear Physics Laboratory, Faculty of Science, University of Yaoundé I, Yaoundé P.O. Box 812, Cameroon; gondjidieusouffit@yahoo.fr
[2] Research Centre for Nuclear Science and Technology (CRSTN), Institute of Geological and Mining Research (IRGM), Yaoundé P.O. Box 4110, Cameroon; bobbomodibo@gmail.com
[3] Institute of Radiation Emergency Medicine, Hirosaki University, 66-1 Honcho, Hirosaki 036-8564, Japan; tokonami@hirosaki-u.ac.jp
[4] Argonne National Laboratory, Environmental Science Division, 9700 S. Cass Avenue, Lemont, IL 60439, USA; dlepoire@anl.gov
* Correspondence: saidous2002@yahoo.fr

Simple Summary: This paper assesses radiation doses in biota and the health risk from exposure to naturally occurring radionuclides in contaminated soil following mining activities at the Nkamouna-Kongo cobalt–nickel deposit. The activity of ^{226}Ra, ^{232}Th, and ^{40}K was determined by γ-spectrometry. The internal doses were 2.13×10^{-07}, 1.42×10^{-06}, and 8.38×10^{-05} Gy d^{-1} for animals and 2.38×10^{-07}, 2.04×10^{-06}, and 9.07×10^{-05} Gy d^{-1} for plants. These values are below the value limit recommended by the US DOE. The maximum total dose of 0.7234 mSv yr^{-1} was obtained at t = 1 year. The external dose contribution obtained at t = 1 year for all nuclides summed and all component pathways was 0.4 mSv yr^{-1}, above the background radiation dose limit of 2.5×10^{-01} mSv yr^{-1}. A maximum cancer risk of 1.36×10^{-03} was observed at t = 1 year. The use of a 1 m cover thickness would remediate the contaminated site to a dose on the order of 10^{-5} mSv yr^{-1} for a period of 0 to 100 years.

Abstract: Nkamouna-Kongo is a cobalt–nickel deposit located in Lomié, Eastern Cameroon. Mining creates radiation exposure pathways that must be considered in risk management scenarios. RESRAD-ONSITE and RESRAD-BIOTA, developed by the US DOE, assess contaminated sites by deriving cleanup criteria and estimating the radiation dose and risk associated with residual radioactive materials using site-specific parameters. This paper evaluated the radiation dose in biota and the health risk from exposure to naturally occurring radionuclides. The activity of ^{226}Ra, ^{232}Th, and ^{40}K was determined by γ-spectrometry. The internal doses were 2.13×10^{-07}, 1.42×10^{-06}, and 8.38×10^{-05} Gy d^{-1} for animals and 2.38×10^{-07}, 2.04×10^{-06}, and 9.07×10^{-05} Gy d^{-1} for plants. The maximum total dose of 0.7234 mSv yr^{-1} was obtained at t = 1 year. The external dose contribution obtained at t = 1 year for all nuclides summed and all component pathways was 0.4 mSv yr^{-1}, above the background radiation dose limit of 2.5×10^{-01} mSv yr^{-1}. A maximum cancer risk of 1.36×10^{-03} was observed at t = 1 year. It was also shown in the RESRAD calculations that the total cancer morbidity risks from plant ingestion, radon (independent of water), and external gamma exposure pathways were greater than those from other exposure pathways. The high risk calculated for ^{226}Ra relative to ^{232}Th and ^{40}K makes it the primary human health concern in the study area. The use of a 1 m cover thickness would remediate the contaminated site to a dose on the order of 10^{-5} mSv yr^{-1} for a period of 0 to 100 years. The values of these doses are below the US DOE recommended limits.

Keywords: RESRAD; cancer risk; contaminated site

Citation: Dieu Souffit, G.; Saïdou; Bobbo Modibo, O.; Lepoire, D.; Tokonami, S. Risk Assessment of Exposure to Natural Radiation in Soil Using RESRAD-ONSITE and RESRAD-BIOTA in the Cobalt-Nickel Bearing Areas of Lomié in Eastern Cameroon. *Radiation* **2022**, *2*, 177–192. https://doi.org/10.3390/radiation2020013

Academic Editor: Michele Guida

Received: 23 February 2022
Accepted: 17 April 2022
Published: 19 April 2022

1. Introduction

Artisanal and industrial mining activities cause more harm than good to the environment despite being one of the best sources of income and wealth creation [1,2]. Several studies have documented serious environmental impacts of mining activities over the past decades worldwide [3–6]. However, it is difficult to identify the main trends in impacts, as human, social, and geographical situations differ so much. Mining in developing countries continues to pose serious environmental issues. The location of mines, unaccountable extraction processes, and the lack of enforcement of mining codes are all factors that make mining an environmental disaster [7,8]. Nkamouna-Kongo is a cobalt–nickel deposit located in the locality of Lomié in the forestry and mining region of Eastern Cameroon. During the mining process, naturally occurring long-lived primordial radionuclides, which exist in trace amounts in all rock and soil formations and represent the main source of external radiation to the public, are fragmented underground and transported to the ground's surface [9]. X-rays, gamma rays, and alpha and beta particles are all forms of ionizing radiation. If present at sufficient levels, they can harm the health of humans and other animals. Scientific studies conducted after the Fukushima disaster have revealed the consequences of radioactivity in living organisms, particularly in wildlife. Exposure of biota to radiation from exploration and mining is of concern because radionuclide concentrations at the surface of the ground can increase during exploration and mining [10]. Thus, exploration and mining can create pathways of radiation exposure that must be considered in risk management scenarios [11]. The mining industry, which is mainly focused on the extraction of minerals and metals, such as iron, copper, cobalt, nickel, and cadmium, degrades ecosystems and contaminates the environment [12–15]. Air contamination can occur through dust released by mining activity and is a serious cause of diseases, usually respiratory disorders, in people and asphyxiation in plants and trees [16,17]. On the other hand, there may be emanations of toxic gases and vapors and the production of sulfur dioxide. Mining activities contribute to the degradation of flora and fauna, the deterioration of the landscape, and the pollution of water resources [18]. The awareness of the need for mining rehabilitation is recent. Many sites are still abandoned after exploitation. Good management of rehabilitation can mitigate and even solve the problem of contamination. In this context, RESRAD, a sustainability assessment tool, has been developed as an instrument to assess the sustainability of the rehabilitation of contaminated areas [19,20].

The RESRAD-ONSITE and RESRAD-BIOTA codes developed by the US DOE were designed to evaluate contaminated sites [21]. They are used to derive clean-up criteria and estimate the radiation dose and risk associated with residual radioactive materials using site-specific parameters. Assessment of the potential radiation impact of environmental contamination with radionuclides in order to prevent or reduce radiation effects in living organisms requires the assessment of radiation doses. Soil and surface water are the pathways by which radionuclides enter the biological systems of biota [22]. The transfer parameter from the soil to the plant is based on the existence of a relationship between the presence of the radionuclide in the soil and the plants [23].

The aim of this work was to assess radiation risk from the Naturally Occurring Radioactive Materials (NORM) on members of the public and biota in the cobalt-, nickel-, and manganese-bearing areas of Nkamouna-Kongo. The entry parameters, namely the activity concentrations of ^{238}U, ^{232}Th, and ^{40}K in the soil, to run RESRAD-ONSITE and RESRAD BIOTA codes were determined using an HPGe spectrometer. These parameters were used to calculate risks factors, such as the sum ratio factor, internal dose rate, external dose rate, and total dose rate in terrestrial plants and terrestrial animals. This study is also a preliminary part of a major environmental radioactivity monitoring campaign in the area of the Nkamouna-Kongo cobalt–nickel–manganese deposit.

2. Materials and Methods

2.1. Study Area

The Lomié subdivision is located in the administrative region of East Cameroon between the latitude of 3°10′ north and the longitude of 13°37′ east (Figure 1). It has about 18,952 inhabitants, including 4266 in the town of Lomié [24]. The relief is hilly with flat valleys in some places, and the altitude of the region is 624 m on average. The climate is humid equatorial with a relative humidity of 77% [25]. Lomié has very favorable soil for agricultural and livestock activities. The main activities of the inhabitants are farming, livestock, fishing, and gathering. The average annual rainfall is 778.4 mm, and the average annual temperature is 23.5 °C. The soils are ferralitic with red facies, sometimes ochre to yellow, not very thick, and stony. In some places, they are gravelly or lateritic. In the talwegs, especially at the edges of watercourses, hydromorphic soils are found, alternating with deposits of sand, laterite, and stones that can be used for various construction works. On the whole, the pedological structure of the area is based on metamorphic rocks (schists, gneiss, orthogneiss, granites, and migmatites rich in kaolinite, goethite, gibbsite, and quartz). We also noted the presence of amphibolites and diorites [26].

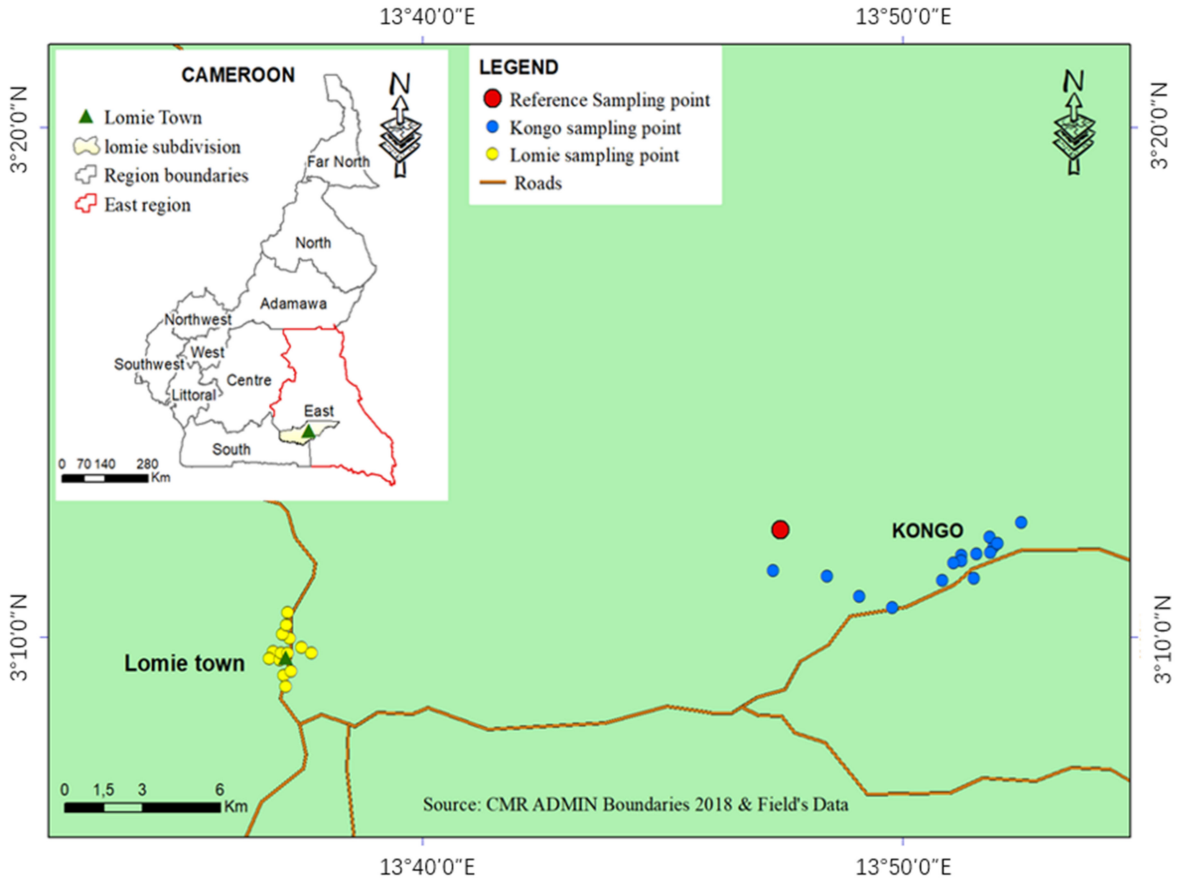

Figure 1. Map of the study area showing the sampling points in Kongo, where the cobalt–nickel deposit is located, and in Lomié, the most populated locality of the area.

Indeed, Lomié is the epicenter of mining in the eastern region. This mining is also accompanied by logging. Far from the mining sites, subsistence family farming, fishing, handicrafts, and small-scale business are carried out, all of which are closely linked to mining activities. Finally, artisanal hunting is also highly developed. Because of the exploration activities carried out by mining companies, the locality of Lomié and its surroundings are experiencing unprecedented pollution.

A study on the assessment of trace element pollution and its potential health risks in the same area was conducted by Gondji et al. (2022) [4]. This study found that high

spatial heterogeneity in trace element concentration was observed in samples from the study area. This variability revealed that samples collected in close proximity to the cobalt–nickel deposit were subject to high trace element concentrations. An assessment of the risk to human health due to exposure to trace elements was also performed [4]. Indeed, the population carcinogenic risk from ingestion exposure was high (2.5×10^{-03}), while the risk from skin exposure was moderate (7.08×10^{-04}) and the risk from inhalation was low (2.50×10^{-07}). In addition, the non-carcinogenic risk for children and adults depends on the metals and their route of exposure.

2.2. Sample Collection and Measurements

Thirty (30) different soil samples were collected at the cobalt exploration site and in the nearby town of Lomié (Figure 1). A random method was chosen for soil sampling. The samples were taken on a surface of 1 m^2 with a depth between 0 and 10 cm and a dry mass of about 500 g. Fifteen soil samples were analyzed at the Research Center for Nuclear Science and Technology of the Institute of Geological and Mining Research (IRGM) (Cameroon) using an NaI (Tl) detector (Model 802) with a crystal size of 7.6 cm × 7.6 cm, a multiple channel analyzer of 1024 channels, and a resolution of 7.5% at 662 keV. The detector was mounted inside a cylindrical lead shielding. The acquisition and analysis of the spectra were performed with the software GENIE 2000 (Canberra). The spectrometer was calibrated using a 500 mL Marinelli Beaker with resin containing ^{155}Eu, ^{60}Co, ^{137}Cs, and ^{22}Na traceable to international standards and emitting gamma-rays in the 60.0–1115.5 keV energy range. The same geometry was used with a counting time of 100,000 s to measure radioactivity in soil samples. The full energy peaks of interest for ^{214}Bi (1120.3 keV and 1764.5 keV) were considered to determine the ^{238}U activity concentration after reaching secular equilibrium between ^{226}Ra and daughter products. The full energy peaks of interest for ^{228}Ac (338.8 keV, 409.5 keV, and 911.6 keV or 969.6 keV, depending on the sample) were considered to determine the ^{232}Th activity concentration. The specific full energy peak of 1460.8 keV of ^{40}K was used to determine its activity concentration [27].

The remaining 15 samples were sent for radioactivity measurement to the Institute of Radiation Emergency Medicine, Hirosaki University, Japan. All measurements were performed using an HPGe detector (GEM40190, AMETEK ORTEC, Oak Ridge, TN, USA) with a relative efficiency of 30% and an energy resolution of 1.85 keV (FWHM) at 1.33 MeV of ^{60}Co using an MCA-7 multichannel analyzer, Seiko EG&G, Japan. The acquisition and analysis of the spectra were performed with GAMMA VISION software (Seiko EG&G, Tokyo, Japan). Radioactivity measurements in soil samples were carried out over a period of 172,800 s (48 h). The sample container had a standard cylindrical shape of the U-8 type (diameter = 48 mm; height = 58 mm) (PURATUBO 3–20 type 100 cm^3 U8, AS ONE, Yamayu, Japan). The samples were dried at 110 °C for 24 h and sieved with 2 mm mesh; about 100 g of sieved sample was placed in a U-8, hermetically sealed with adhesive glue, and stored for 45 days. Energy and detector efficiency calibrations were performed using standard gamma sources provided by the Japan Radioisotope Association with gamma energies ranging from 60 to 1333 keV and an overall uncertainty of less than 10%.

2.3. RESRAD Simulation and Output Parameters

2.3.1. RESRAD-BIOTA

The RESRAD-BIOTA code is used for the assessment of radiological risk to non-human biota. RESRAD-BIOTA version 1.8 was used to estimate the BCG values, total dose, and sum ratio factor in this study. RESRAD-BIOTA offers the necessary capabilities to evaluate the doses received by the biota. The RESRAD-BIOTA code is used to calculate radiation doses in aquatic, sediment, and terrestrial biota. In this work, the organisms studied were grass (terrestrial plants) and terrestrial animals, such as the goats and sheep in the study area, which are of dwarf breeds and have an average weight of about 25 kg [28]. The dose calculation in RESRAD-BIOTA is based on dose conversion factors [29,30]. DCFs are calculated using the Monte Carlo n-particle transport (MCNP) code. In the current study,

assuming a uniform distribution of radionuclides in the body, organisms are represented by a three-dimensional ellipsoidal phantom [31]. RESRAD-BIOTA offers, at its 3rd level, 8 predefined geometries for the terrestrial environment. For this purpose, geometry 6 was used in the present work in order to simulate site-specific terrestrial animals. Since it is possible to vary the mass of the organisms, we used a mass of 25 kg, representing the average mass of mammals in Cameroon [28]. It should be noted that the maximum values of the activity concentrations were used as input values in the RESRAD codes and that, because of secular equilibrium, the concentrations of the progeny were the same as those of the primordial radionuclides.

2.3.2. Equations and Models for Terrestrial Systems

1. Soil BCGs for Terrestrial Plants

Biota Concentration Guide (*BCG*) is the limiting concentration of a radionuclide in the soil, sediment, or water that would not cause the dose rate criteria for the protection of populations of aquatic and terrestrial biota to be exceeded [31]. The method used to derive the BCGs for terrestrial plant exposure to a single nuclide in contaminated soil is:

$$BCG_{soil,\ terrestrial\ plant,\ i} = \frac{365.25 \times \mathrm{DL}_{tp}}{CF_{tp} \times \left[\left(B_{iv,tp,i} \times DCF_{int,i}\right) + DCF_{ext,i,sol}\right]} \quad (1)$$

where:

- $BCG_{soil,\ terrestrial\ plant,\ i}\ \left[\frac{Bq}{kg}\right]$ is the nuclide concentration i in the soil;
- $B_{ivtp,soil,i}$ is the concentration factor of the fresh mass of the terrestrial plant in the soil for nuclide i;
- $B_{iv,tp,i}$ is the concentration factor of the fresh mass of the land plant with respect to the soil;
- CF_{tp} is the correction factor for area or time;
- DL_{tp} (0.01 Gy d^{-1}) is the dose limit recommended for terrestrial plants;
- $DCF_{ext,soil,i}\ \left[\frac{\mathrm{Gy/y}}{\mathrm{Bq/kg}}\right]$ is the dose conversion;
- $DCF_{int,}\ \left[\frac{\mathrm{Gy/y}}{\mathrm{Bq/kg}}\right]$ is the dose conversion factor.

2. Soil BCGs for Terrestrial Animals

The method used to derive the terrestrial animal BCGs for exposure to a single nuclide in contaminated soil is:

$$BCG_{soil,\ terrestrial\ animal,\ i} = \frac{365.25 \times \mathrm{DL}_{ta}}{CF_{ta} \times \left[\left(B_{iv,ta,i} \times DCF_{int,i}\right) + DCF_{ext,i,sol}\right]} \quad (2)$$

where:

- DL_{ta} (0.01 Gy d^{-1}) is the dose limit recommended for terrestrial animals;
- $BCG_{soil,\ ta,\ i}\ \left[\frac{Bq}{kg}\right]$ is the concentration of nuclide i in the soil;
- $B_{iv,ta,i}$ is the concentration factor of the fresh mass of land animals in relation to the soil.

3. Sum Ratio Factor (SRF)

The SFR is the value of the absorbed dose rate in biota relative to the total dose limit in biota. DOE reports show that the absorbed dose limits in biota are 10 m Gy d^{-1} for aquatic animals and terrestrial plants and 1 m Gy d^{-1} for terrestrial and riparian animals [31]. The following relationship gives the expression of SFR:

$$\mathrm{SFR} = \frac{dose\ in\ biota}{dose\ limit} \quad (3)$$

where the dose to biota is measured in Gy d^{-1}, and the dose limit value is based on international standard DOE reports (Gy d^{-1}). Table 1 presents the DOE dose rate criteria used in the calculation of the RESRAD for terrestrial plants and terrestrial animals.

Table 1. DOE dose rate criteria.

	Dose Rate Limit (Gy d^{-1})
Terrestrial Plants	0.01
Terrestrial Animals	0.001

In addition, the internal dose rate, the external dose rate, and the total dose rate due to concentrations of the various radionuclides in the soil were estimated by the RESRAD code. The formulas describing external and internal doses were described by Higley et al. [32].

2.3.3. RESRAD-ONSITE

Version 7.2 of the RESRAD-ONSITE code was used to assess the cancer risk of exposure to natural radionuclides in the soil around the Lomié high-potential mining site, which covers an area of 15,000 m^2 and is 0.1 m thick. The site-specific parameters used in this study are listed in Table 2.

Table 2. Site-specific parameters of the study area.

Parameters	**Site-Specific Data**
Area of contaminated zone	15,000 m^2
Thickness of contaminated zone	0.1 m
Cover depth	1 m
Density of contaminated zone	1.4 cm^3 g^{-1}
Wind speed	1.67 m s^{-1}
Precipitation rate	0.7784 m yr^{-1}
Well pump intake	15 m
Indoor time factor	0.6
Outdoor time factor	0.4

All other parameters are used as default values. However, it should be noted that the distribution coefficients (kds) of natural primordial radionuclides (^{238}U, ^{232}Th, ^{226}Ra, and ^{40}K) were set at 15 cm^3 g^{-1}, 3300 cm^3 g^{-1}, 36,000 cm^3 g^{-1}, and 55 cm^3/g, respectively, for loamy soils in order to assess the mechanism of transport to the water table [33].

3. Results and Discussion

3.1. Activity Concentrations of Natural Primordial Radionuclides (^{226}Ra, ^{232}Th, and ^{40}K)

The activity concentrations of ^{226}Ra, ^{232}Th, and ^{40}K for the thirty (30) soil samples (Table 3) were compared to the world average activity concentrations as well as the results of studies conducted in Batouri and Betaré-Oya, located in the same region. Thus, these results clearly show that the radioactivity levels of ^{226}Ra and ^{232}Th are in the same range as the global average; however, radioactivity levels of ^{40}K were below the global average [9]. The highest activity concentrations for ^{232}Th were found in the samples taken in the vicinity of the cobalt–nickel high-potential mining site, whereas those for ^{40}K and ^{226}Ra were found in the samples taken in Kongo, a village located at about 2 km from the cobalt–nickel high-potential mining site.

Table 3. Activity concentrations in soil samples of ^{226}Ra, ^{232}Th, and ^{40}K measured with the NaI (Tl) and HPGe detectors.

Activity Concentration ($Bq \cdot kg^{-1}$)	With the NaI (Tl) Detector			With the HPGe Detector		
	Radionuclides					
	^{226}Ra	^{232}Th	^{40}K	^{226}Ra	^{232}Th	^{40}K
Minimum	34 ± 18	58 ± 5	45 ± 1	19 ± 1	45 ± 1	158 ± 5
Maximum	53 ± 28	126 ± 17	339 ± 8	63 ± 1	50 ± 1	463 ± 7
Mean	45 ± 23	87 ± 11	135 ± 3	35 ± 1	42 ± 1	215 ± 5
World average	33	45		420		
Batouri average	46	32		76		
Betaré-Oya average	32	37		197		

The reported activity concentrations of ^{226}Ra, ^{232}Th, and ^{40}K in soil samples from the gold mining areas of Betaré-Oya ranged from 29 to 63 $Bq \cdot kg^{-1}$, 13 to 87 Bq kg^{-1}, and 16 to 414 Bq kg^{-1} with mean values of 32 ± 7 Bq kg^{-1}, 37 ± 13 Bq kg^{-1}, and 197 ± 21 Bq kg^{-1} for ^{226}Ra, ^{232}Th, and ^{40}K, respectively [34]. In addition, activity concentrations reported in soil samples from the gold mining areas of Batouri ranged from 32 to 62 Bq kg^{-1}, 22 to 40 Bq kg^{-1}, and 41 to 115 Bq kg^{-1} with mean values of 46 Bq kg^{-1}, 32 Bq kg^{-1}, and 76 Bq kg^{-1}, respectively, for ^{226}Ra, ^{232}Th, and ^{40}K [34].

These results show that the radioactivity level in the current study area for ^{40}K was slightly lower than those at the gold mining sites of Batouri and Betaré-Oya, and the radioactivity levels for ^{226}Ra and ^{232}Th were slightly higher [34].

A statistical comparison of two sets of samples was made. The *p*-values were calculated for comparison purposes. Firstly, the activity concentrations obtained for the immediate vicinity of the mining site (disturbed area by mineral exploration) were compared with those obtained at Lomié (undisturbed area). The activity concentrations of ^{40}K, ^{232}Th, and ^{226}Ra in the samples taken at Lomié varied from 77 to 212 Bq kg^{-1}, 54 to 97 Bq kg^{-1}, and 34 to 50 Bq kg^{-1}, respectively, with arithmetic means of 140 Bq kg^{-1}, 74 Bq kg^{-1}, and 44 Bq kg^{-1}, respectively. At the disturbed area, the activity concentrations ranged from 46 to 340 Bq kg^{-1}, 40 to 126 Bq kg^{-1}, and 36 to 54 Bq kg^{-1}, respectively, for ^{40}K, ^{232}Th, and ^{226}Ra with arithmetic means of 158 Bq kg^{-1}, 86 Bq kg^{-1}, and 46 Bq kg^{-1} respectively. A t-test was performed, and a *p*-value of 0.275 was obtained. This result indicates that there was no statistically significant difference between the data obtained in the undisturbed and disturbed areas (p-value > 0.05).

Secondly, the activity concentrations of ^{226}Ra, ^{232}Th, and ^{40}K in the control sampling from an area with no anthropogenic activity were 34 Bq kg^{-1}, 54 Bq kg^{-1}, and 77 Bq kg^{-1}, respectively. The *p*-values calculated to compare the activity concentrations of the area with high mining potential and of Lomié with those of the control sampling area were all equal to zero (p-value = 0). Thus, the radionuclide concentrations in the immediate vicinity of the cobalt site and in Lomié are significantly higher than those in the control sampling area.

Thus, the activity concentrations of radionuclides vary from site to site, which is explained by the non-uniform distribution of radioactive material in the geological matrix. The variation of activity concentrations in the study area could be attributed to two factors: firstly, the differences in the distribution of natural radionuclides in the rocks and soils that make up the geology of the area and the variable deposition of the clay content, which constitutes the formation of the geology of the investigated area; secondly, the soil excavation during the exploration of the cobalt–nickel deposit of Nkamouna-Kongo [35].

3.2. The Biota Concentration Guide (BCG), Sum Ratio Factor (SRF), Internal Dose, External Dose, and Total Dose of Different Radionuclides in Four Organism Types by Soil (Bq kg^{-1}) Media

Calculations using RESRAD-BIOTA version 1.8 software revealed that BCG levels in the soil ranged from $5.10 \times 10^{+04}$ Bq kg^{-1} to $5.49 \times 10^{+03}$ Bq kg^{-1} for ^{40}K; $8.75 \times 10^{+05}$ Bq kg^{-1} to $6.16 \times 10^{+04}$ Bq kg^{-1} for ^{232}Th; and $5.82 \times 10^{+05}$ Bq kg^{-1} to $2.13 \times 10^{+05}$ Bq kg^{-1} for ^{226}Ra. These BCG values represent the limits of radionuclide concentrations in an environmental

medium that will not result in exceeding the standard recommended doses for biota. The SRFs of ^{40}K, ^{232}Th, and ^{226}Ra in soil samples, calculated according to the organism, are presented in Table 4. These results show that the SRF values of ^{40}K were 8.44×10^{-02} for terrestrial animals and 9.07×10^{-03} for terrestrial plants. For the case of ^{232}Th, we obtained a value of 2.04×10^{-03} for terrestrial animals and 1.44×10^{-04} for terrestrial plants; for the case of ^{226}Ra, we obtained a value of 2.44×10^{-04} for terrestrial animals and 8.93×10^{-05} for terrestrial plants. The total ratio factors (SFRs) for the different radionuclides met the requirement that this factor be ≤ 1 [21]. Figure 2a shows the total SFR in soil media.

Table 4. The biota concentration guide (BCG), sum ratio factor (SRF), internal dose, external dose, and total dose of ^{226}Ra, ^{232}Th, and ^{40}K in two organism types by soil (Bq kg^{-1}) media.

Risk Parameter	Radionuclides	Terrestrial Animal	Terrestrial Plant
Sum ratio factor $\left(\frac{\text{dose in biota}}{\text{dose limit}}\right)$	^{226}Ra	2.44×10^{-04}	8.93×10^{-05}
	^{232}Th	2.04×10^{-03}	1.44×10^{-04}
	^{40}K	8.44×10^{-02}	9.07×10^{-03}
Biota Concentration Guide (BCG) (Bq kg^{-1})	^{226}Ra	$2.13 \times 10^{+05}$	$5.82 \times 10^{+05}$
	^{232}Th	$6.16 \times 10^{+04}$	$8.75 \times 10^{+05}$
	^{40}K	$5.49 \times 10^{+03}$	$5.10 \times 10^{+04}$
External dose (Gy d^{-1})	^{226}Ra	1.34×10^{-08}	6.55×10^{-07}
	^{232}Th	1.65×10^{-10}	2.21×10^{-08}
	^{40}K	6.18×10^{-07}	4.32×10^{-06}
Internal dose (Gy d^{-1})	^{226}Ra	2.31×10^{-07}	2.38×10^{-07}
	^{232}Th	2.04×10^{-06}	1.42×10^{-06}
	^{40}K	8.38×10^{-05}	8.64×10^{-05}
Total dose (Gy d^{-1})	^{226}Ra	2.44×10^{-07}	8.93×10^{-07}
	^{232}Th	2.04×10^{-06}	1.44×10^{-06}
	^{40}K	8.44×10^{-05}	9.07×10^{-05}

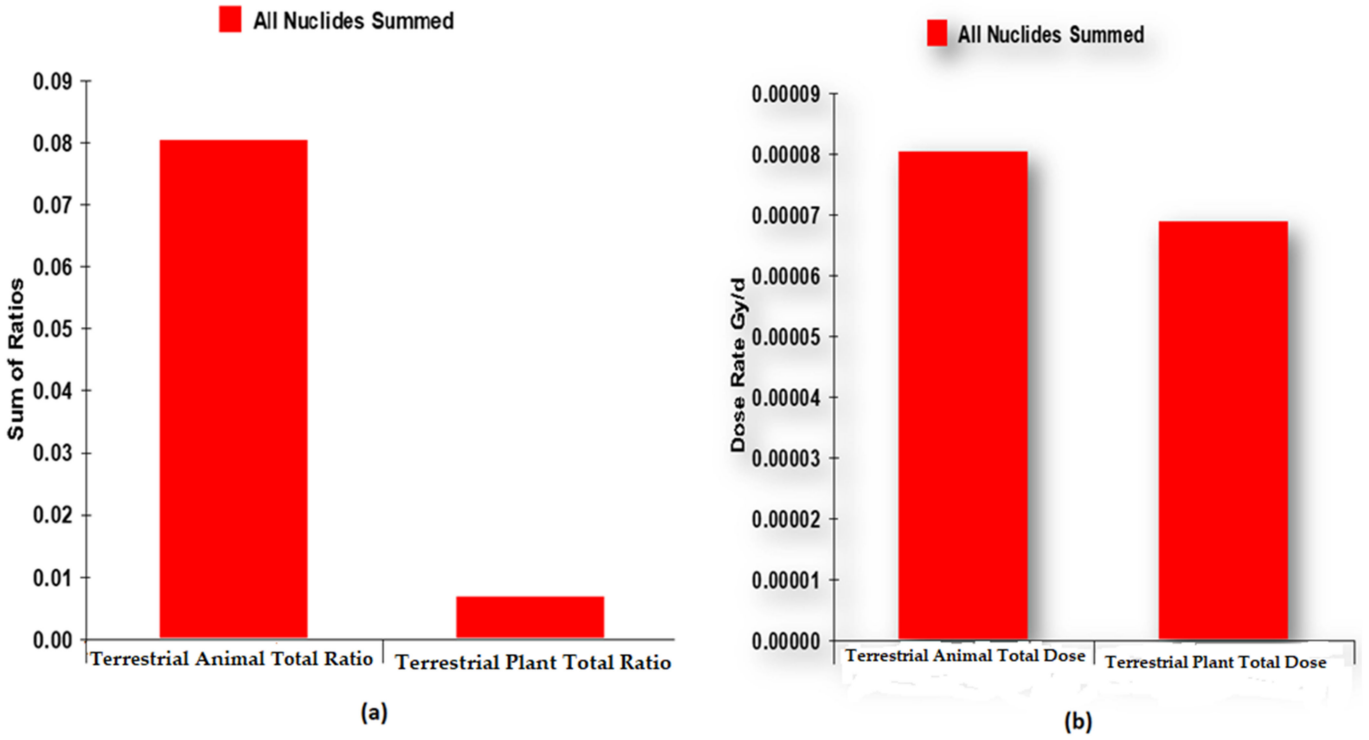

Figure 2. Sum Ratio Factor (SRF) (**a**) and total dose rate (**b**).

The external dose rates for terrestrial plants due to exposure to ^{226}Ra, ^{232}Th, and ^{40}K were 6.55×10^{-07} Gy d^{-1}, 2.21×10^{-08} Gy d^{-1}, and 4.32×10^{-06} Gy d^{-1}, respectively, and those for terrestrial animals were 1.34×10^{-08} Gy d^{-1}, 1.65×10^{-10} Gy d^{-1}, and 6.18×10^{-07} Gy d^{-1} due to exposure to ^{226}Ra, ^{232}Th, and ^{40}K respectively.

Similarly, the internal dose rate value in the soil of the study area due to exposure to ^{226}Ra was 2.13×10^{-07} Gy d^{-1} for terrestrial animals and 2.38×10^{-07} Gy d^{-1} for terrestrial plants; as for ^{232}Th, a value of 2.04×10^{-06} Gy d^{-1} was obtained for terrestrial animals and 1.42×10^{-06} Gy d^{-1} for terrestrial plants. For the case of ^{40}K, we obtained a value of 8.38×10^{-05} Gy d^{-1} for terrestrial animals and 9.07×10^{-05} Gy d^{-1} for terrestrial plants. These dose rate values are below the US DOE's recommended dose limits. These results indicate that the dose rates may not pose a threat to terrestrial animal and plant populations in the study area.

The total dose rate value due to exposure to ^{226}Ra, ^{232}Th, and ^{40}K was higher for terrestrial animals than terrestrial plants. The dose calculated with RESRAD-BIOTA in this study is below the US DOE standard dose limits. Figure 2b shows the total dose rate in the terrestrial animals and terrestrial plants for all nuclides summed.

3.3. Environmental Risk

The aim of dose and risk assessment is to produce a more accurate estimation of the risk from a contaminated site in order to understand the level of the risk.

The following results (Figures 3–8) are those obtained with RESRAD-ONSITE taking a cover depth equal to zero. The cover depth was used later to evaluate the exposure risk when taking a depth of 1 m (Figure 9).

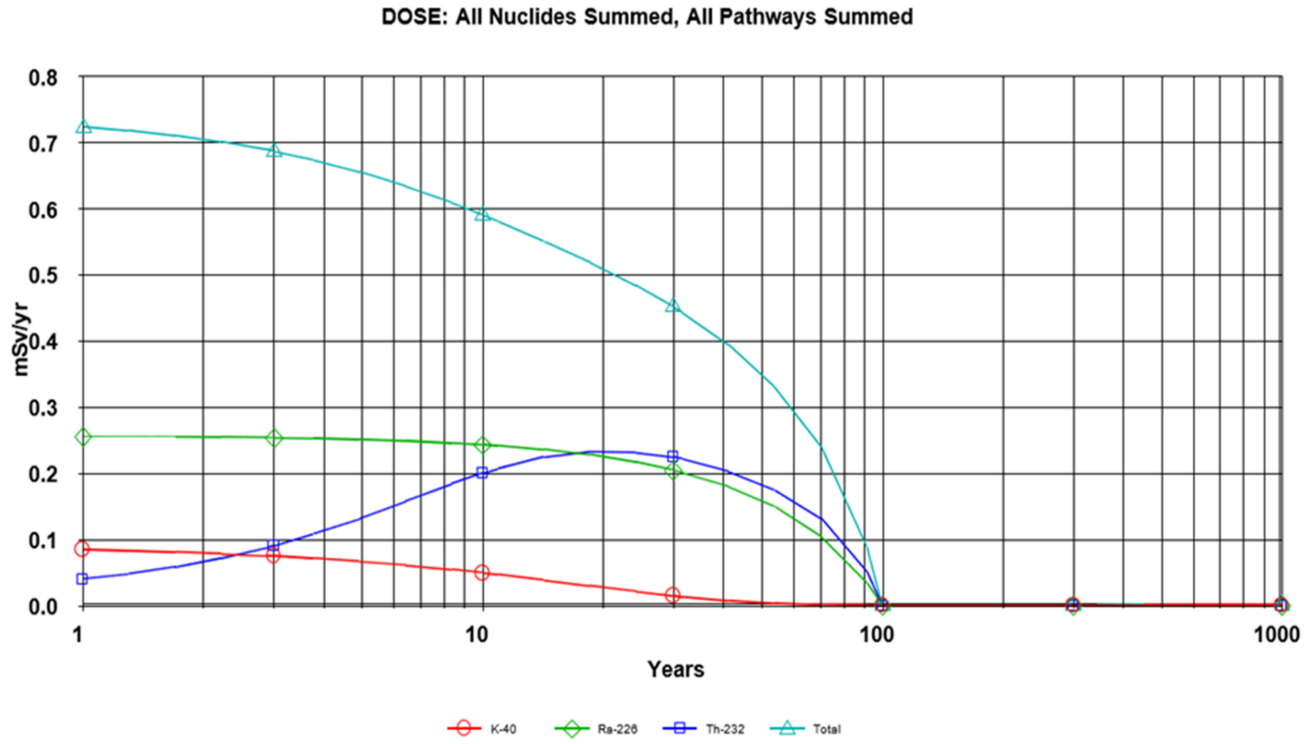

Figure 3. Summed total dose due to all nuclides and all pathways.

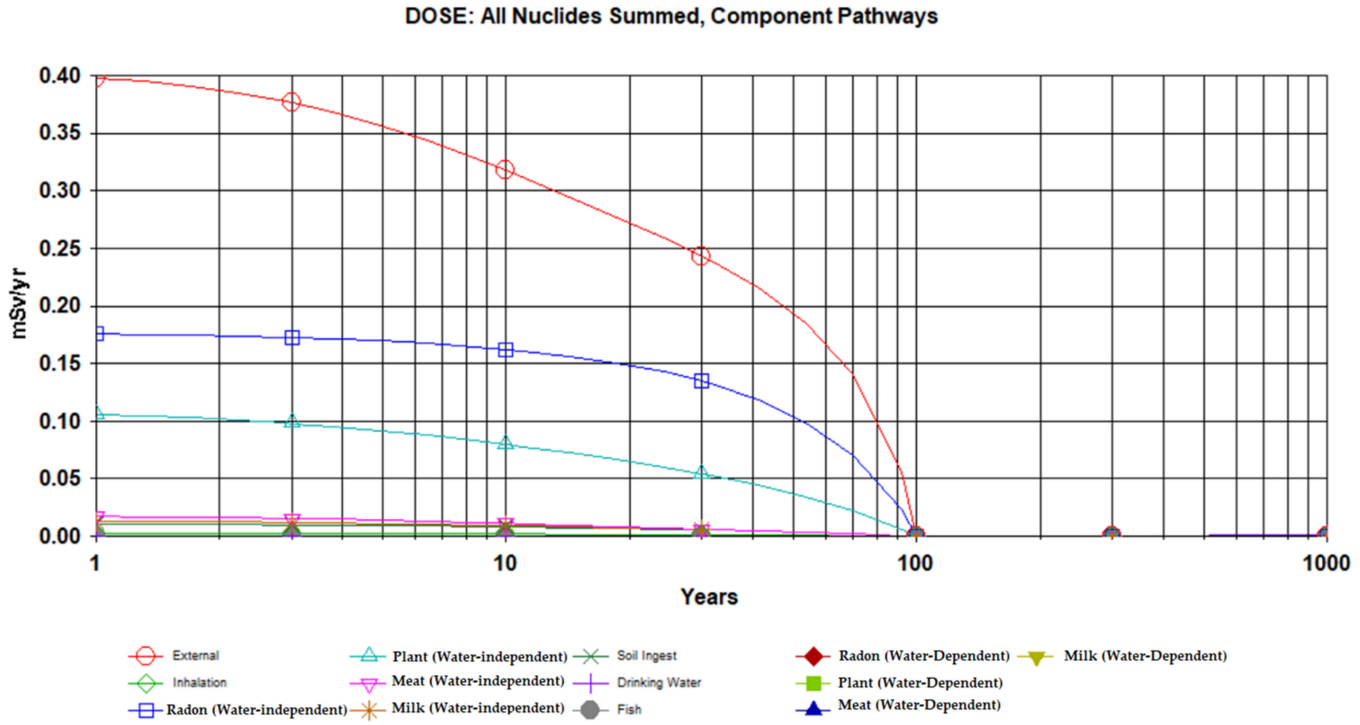

Figure 4. Dose contributions from all nuclides summed and for all exposure pathways.

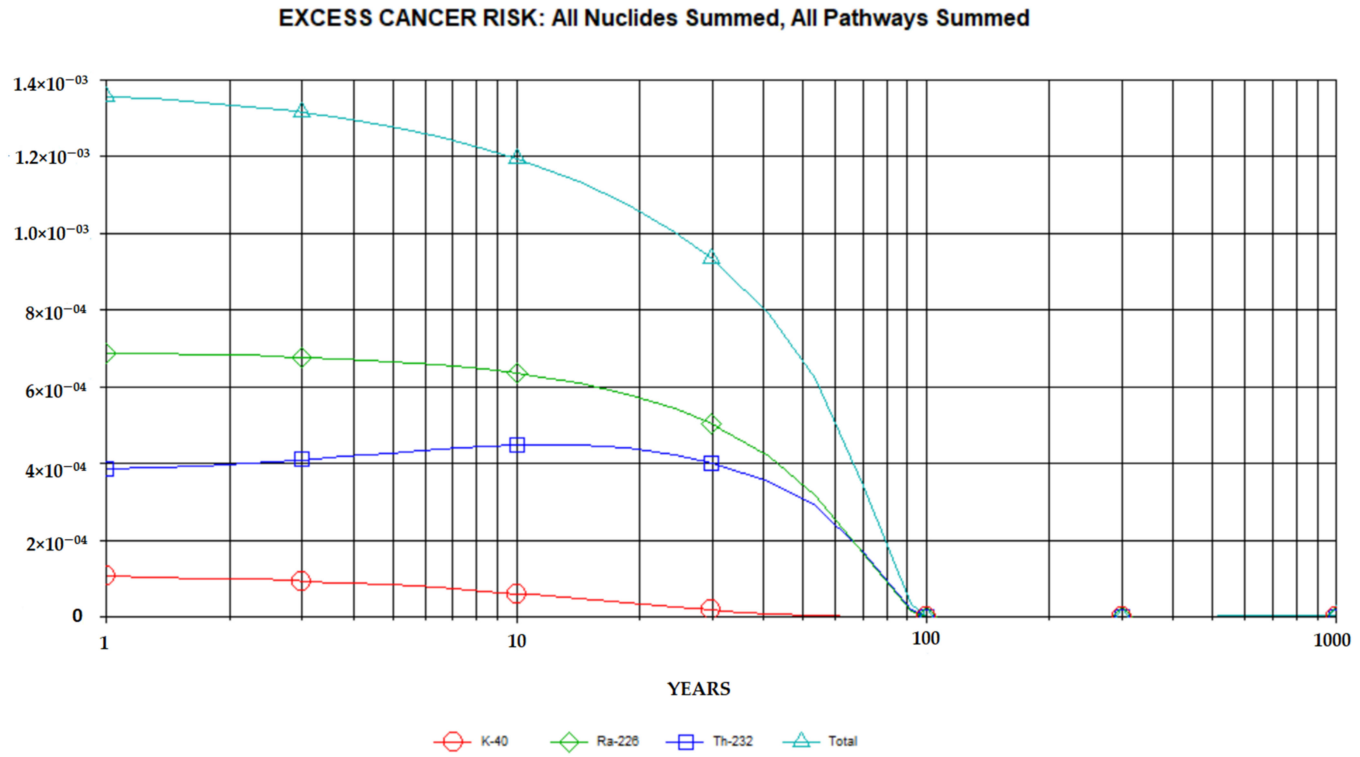

Figure 5. Cancer risk depending on time and contributions from all nuclides.

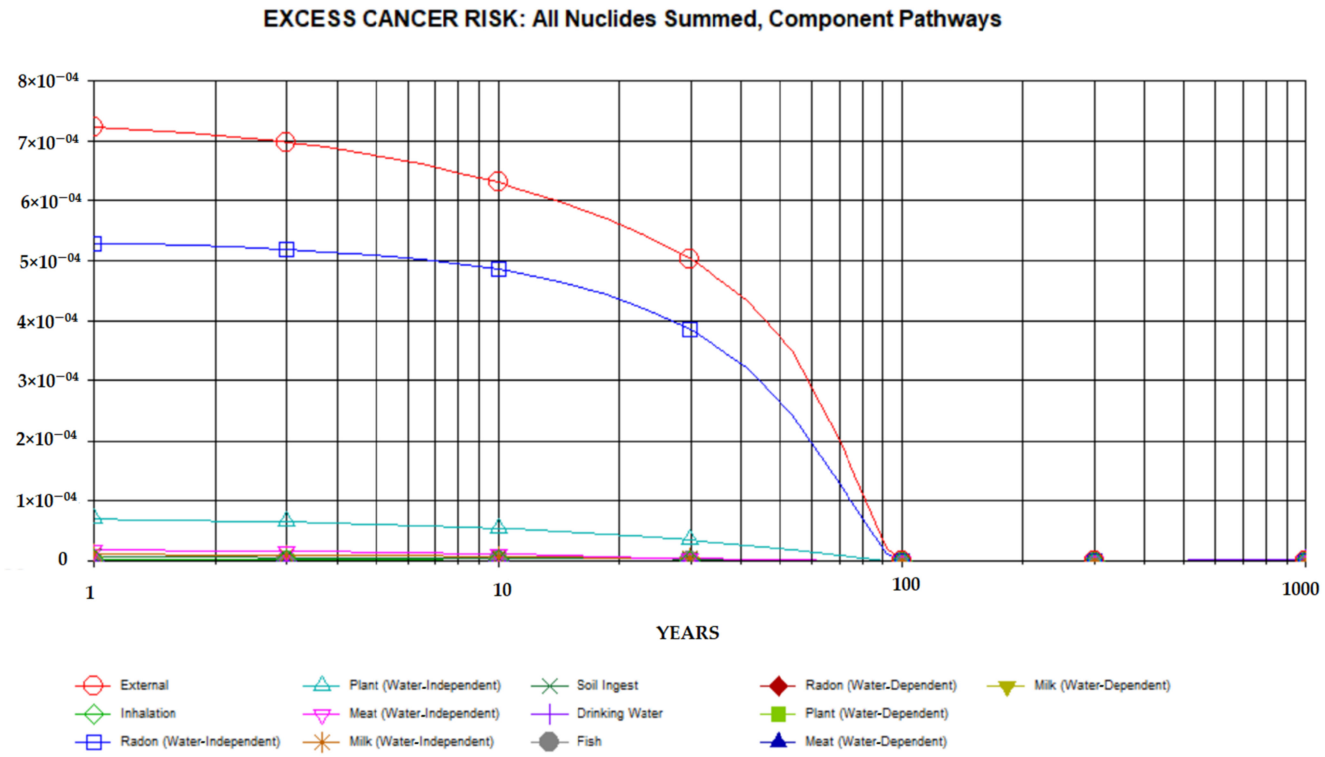

Figure 6. Contributions of exposure pathways to cancer risk.

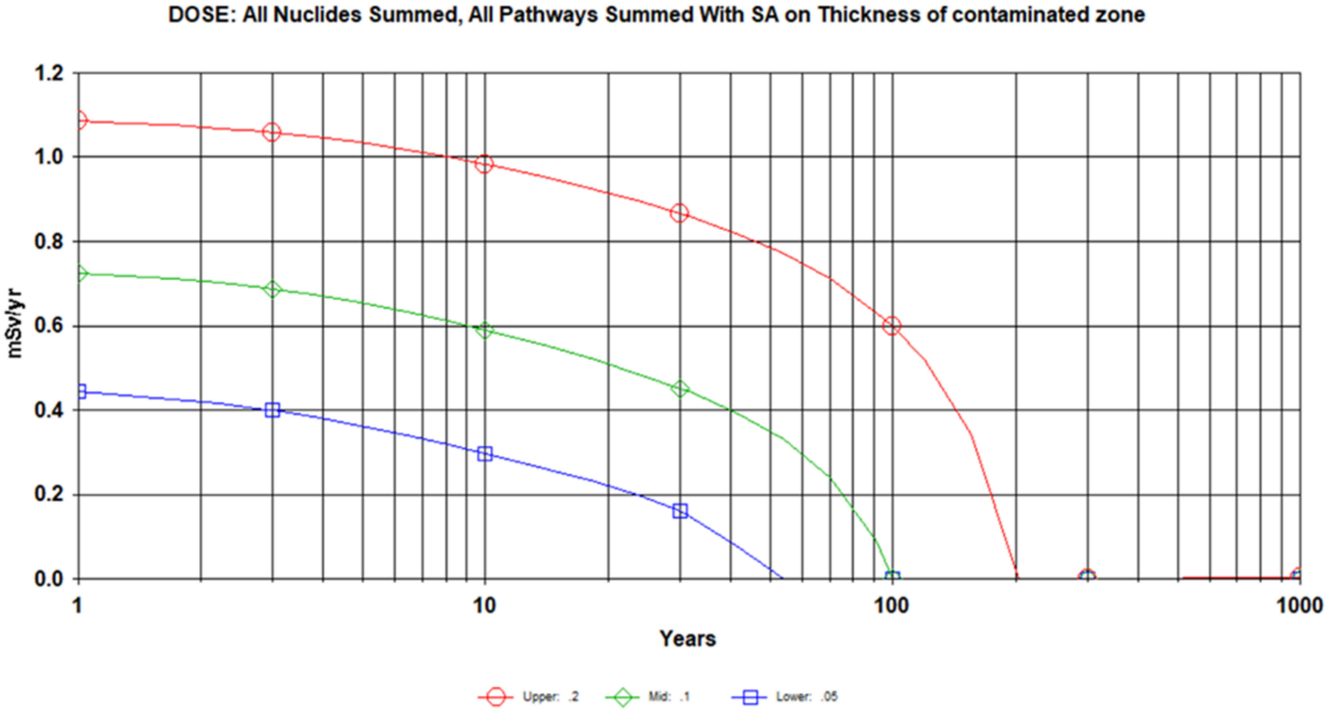

Figure 7. Total dose versus time for all radionuclides summed and all exposure pathways summed taking into account the sensitivity analysis on the thickness of the contaminated area.

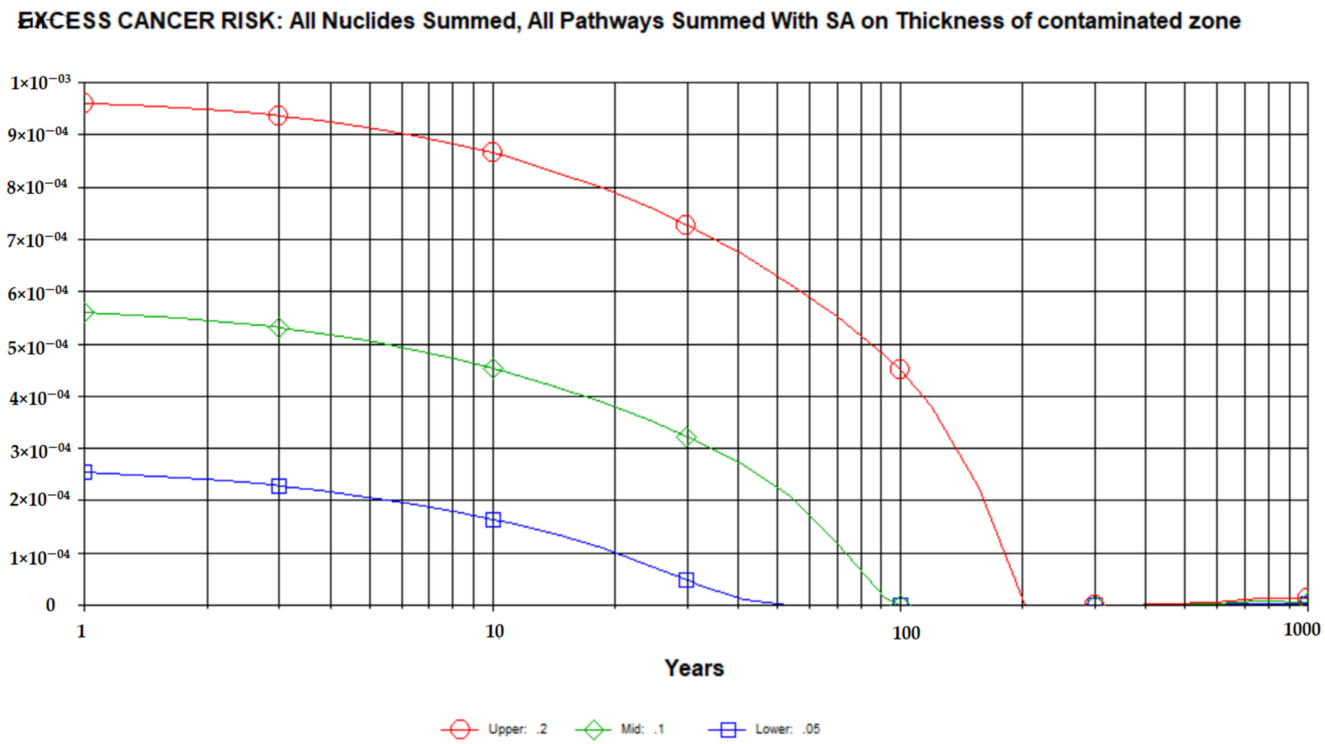

Figure 8. Cancer risk as a function of time for all radionuclides summed and all exposure pathways summed using the sensitivity analysis on the thickness of the contaminated area.

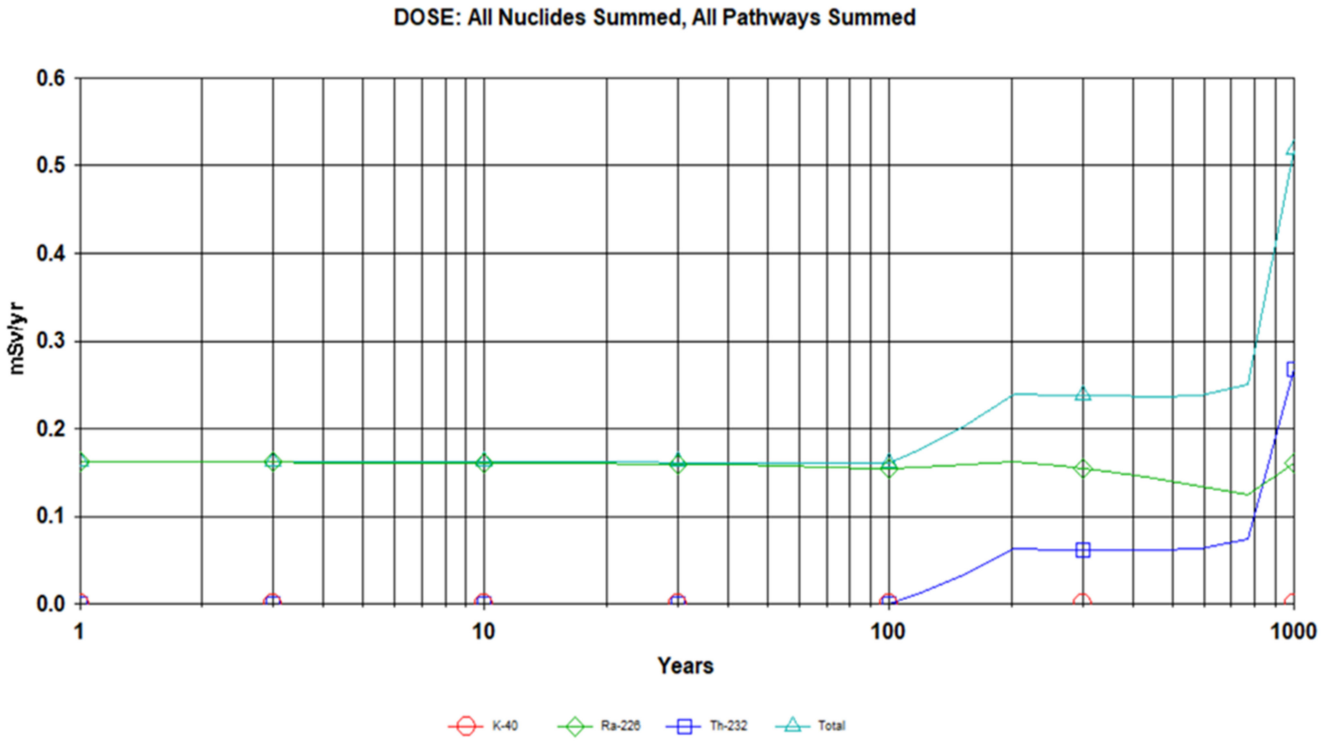

Figure 9. Total dose of all nuclides using a cover thickness of 1 m.

Figure 3 shows the variation in the dose due to ^{40}K, ^{232}Th, and ^{226}Ra over a period of 1000 years due to the mining activity. This figure shows that the maximum total dose due to ^{226}Ra, ^{232}Th, ^{40}K, and their progeny of 0.7234 mSv yr^{-1} was obtained at t = 1 year. Similarly, the total dose contributions calculated with RESRAD-ONSITE for each radionuclide at

t = 1 year for the ground pathway were 0.0827 mSv yr^{-1} for ^{226}Ra, 0.0220 mSv yr^{-1} for ^{232}Th, and 0.0615 mSv yr^{-1} for ^{40}K. The high values of the calculated doses for ^{226}Ra compared with ^{232}Th and ^{40}K make it the main human health concern in the study area.

Similarly, the excess risk and excess effective dose due to natural background radiation (Lomié) were also evaluated. The maximum total dose due to natural background radiation from ^{226}Ra, ^{232}Th, ^{40}K, and their progeny of 0.410 mSv yr^{-1} was obtained at t = 1 year, and the total dose contributions calculated with RESRAD-ONSITE for each radionuclide at t = 1 year for the ground pathway were 0.0733 mSv yr^{-1} for ^{226}Ra, 0.0169 mSv yr^{-1} for ^{232}Th, and 0.0281 mSv yr^{-1} for ^{40}K.

It is clear that the impact of the mining activity (excavation of the ground during exploration) is visible because the results show that the excess effective dose received because of the mining activity was greater than that received in the area representing the natural radiation background (Lomié).

The external dose contribution obtained at t = 1 year for all nuclides summed and all component pathways was 0.4 mSv yr^{-1}. The external pathway is thus the largest contributor to exposure among all the pathways (Figure 4). This dose is above the basic radiation dose limit of 2.5×10^{-01} mSv yr^{-1}. The different values of the dose contributions for each radionuclide are superior to those obtained by Njinga and Tshivhase [36] except for the case of ^{232}Th. It should also be noted that the total dose obtained in this study for all exposure pathways summed at t = 1 year is lower than that obtained by the same authors. This difference could be due to the geology of the study area.

Figure 5 shows the cancer risk assessed with RESRAD-ONSITE. This curve shows that the risk of cancer following exposure to the various radionuclides decreases from the first to the hundredth year for all primordial radionuclides. The risk tends toward zero from the 100th year onwards. The maximum value of the total cancer risk of 1.356×10^{-03} was observed at t = 1 year. It should also be noted that the contribution of ^{226}Ra to cancer risk is high compared with that of ^{232}Th. ^{226}Ra is therefore the major contributor to cancer risk (Figure 5).

Figure 6 shows the variation in cancer risk, taking into account all exposure pathways. The external pathway is the major pathway contributing to cancer risk. There is a decrease in the contribution of all pathways from t = 1 year to t = 100 years. The risk tends toward zero after 100 years.

The cancer risk for inhalation of radon and its progeny at t = 1 year (water-independent pathway) was calculated by RESRAD-ONSITE. It should be noted that RESRAD evaluates the risk of radon and thoron as a function of the concentration of radium and thorium [37]. Given the high concentrations of ^{232}Th in the soil samples from the current study area, the contribution of thoron (^{220}Rn) to cancer risk is high. Thus, the cancer risk of ^{222}Rn is 4.83×10^{-05}; for its decay progeny, the cancer risk is 9.52×10^{-05} for ^{218}Po, 1.21×10^{-04} for ^{214}Pb, and 2.36×10^{-04} for ^{214}Bi. These values are below the limit of 3.00×10^{-4} obtained by using the recommended value of 0.25 mSv/year, except for the values for ^{214}Pb and ^{214}Bi. For ^{220}Rn, the contribution to the cancer risk is 1.80×10^{-05}, and for its decays progeny, the cancer risk is 2.83×10^{-07} for ^{216}Po, 9.90×10^{-06} for ^{212}Pb, and 4.74×10^{-06} for ^{212}Bi. These values are high compared with those for ^{222}Rn because ^{220}Rn is a progeny of ^{232}Th, which has a higher concentration than ^{226}Ra. Note that the contributions to cancer risk from ^{222}Rn and ^{220}Rn are ten times smaller than the limit of 3.00×10^{-4} obtained using the recommended value of 0.25 mSv yr^{-1}. Other studies, such as [38,39], have been conducted on radon, thoron, and thoron progeny in the same region (eastern Cameroon). It appears from these studies that the contribution of thoron to the inhalation dose due to radon and thoron exposure ranges between 7 and 70% in Betare-Oya.

It is important to note that RESRAD cannot be an appropriate model for radon risk assessment because there is no direct input for radon activity concentration in RESRAD [37].

Sensitivity analysis is the study of how uncertainty in the output of a code can be attributed to uncertainty in its inputs. It involves estimating sensitivity indices that quantify the influence of an input or group of inputs on the output. In order to assess the importance

of certain parameters in the risk assessment, a sensitivity analysis was conducted for the thickness of the contaminated area, the variation of which may influence the environmental risk assessment of our study area [37].

Figures 7 and 8 show the variation in dose and cancer risk, respectively. In both cases, it can be seen that if the thickness of the contaminated area is doubled, then the dose and cancer risk increase, and if the thickness is divided by 2, these two parameters decrease. Thus, at t = 1 year, when the thickness is doubled, the cancer risk increases from 1.36×10^{-03} to 2.24×10^{-03}, while when it is divided by 2, the cancer risk decreases from 1.36×10^{-03} to 6.67E−4.

For the purpose of estimating the cleanup level of the contaminated site studied in the current work, a clean cover thickness of 1 m was used. Figure 9 shows the variation of the cumulative dose for all radionuclides with a clean cover thickness of 1 m. This figure shows that using this cover thickness, the dose due to ^{232}Th and ^{40}K is insignificant from t = 0 to t = 100 years. On the other hand, we observed a stable value of the dose equal to 0.16 mSv yr^{-1} due to ^{226}Ra from t = 0 to t = 100 years. This value is lower than the limit value and does not pose any major health risk. For a considerable reduction of the dose and the associated risk, it is thus important to increase the cover thickness. The maximum total dose of 0.52 mSv yr^{-1} was observed at t = 1000 years.

4. Conclusions

Using gamma-ray spectrometry, the activity concentrations of ^{226}Ra, ^{232}Th, and ^{40}K in thirty soil samples collected in the locality of Lomié in Cameroon were determined. These activity concentrations were used as input parameters to run the RESRAD-BIOTA and RESRAD-ONSITE codes to determine the biota concentration guide (BCG), the internal and external dose rate in biota, the sum ratio factor (SFR), and an excess cancer risk assessment. The maximum concentrations of ^{226}Ra, ^{232}Th, and ^{40}K were found to be 52 Bq kg^{-1}, 126 Bq kg^{-1}, and 463 Bq kg^{-1}, respectively. Calculations with RESRAD-BIOTA version 1.8 software revealed that the maximum and minimum biota concentration guide (BCG) levels in the soil for ^{40}K, ^{232}Th, and ^{226}Ra were $5.10 \times 10^{+04}$ Bq kg^{-1} to $4.39 \times 10^{+03}$ Bq kg^{-1}, $8.75 \times 10^{+05}$ Bq kg^{-1} to $5.62 \times 10^{+04}$ Bq kg^{-1}, and $5.82 \times 10^{+05}$ Bq kg^{-1} to $5.84 \times 10^{+04}$ Bq kg^{-1}, respectively. The dose rate values obtained with RESRAD-BIOTA version 1.8 are below the dose limits recommended by the US Department of Energy (DOE). These results indicate that the dose rates may not pose a threat to terrestrial animal and plant populations in the study area. According to RESRAD-ONSITE, the maximum total dose of 0 0.7234 mSv yr^{-1} was obtained at t = 1 year. Furthermore, the total dose contributions calculated with RESRAD-ONSITE for each radionuclide at t = 1 year for the ground pathway were 0.0827 mSv yr^{-1} for ^{226}Ra, 0.0220 mSv yr^{-1} for ^{232}Th, and 0.0615 mSv yr^{-1} for ^{40}K. The external dose contribution obtained at t = 1 year for all nuclides summed and all component pathways was 0.4 mSv yr^{-1}, above the background radiation dose limit of 2.5×10^{-01} mSv yr^{-1}. The maximum value of the total cancer risk of 1.356×10^{-03} was observed at t = 1 year. It should also be noted that the contribution of ^{226}Ra to cancer risk is high compared to that of ^{232}Th. Radium is therefore the major contributor to cancer risk. The use of a cover thickness of 1 m would allow the contaminated site to be remediated to a dose on the order of 10^{-5} mSv yr^{-1} for a period of 1 to 100 years, and the maximum total dose of 0.52 mSv yr^{-1} was observed at t = 1000 years. Therefore, all the data obtained in the present study will help protect humans, animals, and terrestrial plants from the effects of ionizing radiation and provide an idea of the risk of cancer due to natural radionuclide exposure. Environmental assessment is planned during and after mining to demonstrate its impact for better radiological protection of members of the public and the environment.

Author Contributions: Conceptualization, G.D.S. and S.; methodology, G.D.S. and S.; software, G.D.S., O.B.M. and D.L.; validation, G.D.S., S. and D.L.; formal analysis, G.D.S., O.B.M. and S.; investigation, G.D.S. and S.; resources, G.D.S., O.B.M., S. and S.T.; writing—original draft preparation, G.D.S. and S.; writing—review and editing, G.D.S., O.B.M., D.L. and S.; supervision, D.L., S. and S.T.; funding acquisition, S. All authors have read and agreed to the published version of the manuscript.

Funding: This research was funded by the Ministry of Scientific Research and Innovation, Cameroon, through the Public Investment Budget 2019.

Institutional Review Board Statement: Not applicable.

Informed Consent Statement: Not applicable.

Data Availability Statement: The data presented in this study are available in this article.

Conflicts of Interest: The authors declare no conflict of interest.

References

1. Macháček, J. Typology of Environmental Impacts of Artisanal and Small-Scale Mining in African Great Lakes Region. *Sustainability* **2019**, *11*, 3027. [CrossRef]
2. Hilson, G.M. *The Socio-Economic Impacts of Artisanal and Small-Scale Mining in Developing Countries*; CRC Press: Boca Raton, FL, USA, 2003.
3. Jain, R.K.; Cui, Z.; Domen, J.K. *Chapter 4—Environmental Impacts of Mining*; Jain, R.K., Cui, Z.C., Domen, J.K., Eds.; Butterworth-Heinemann: Boston, MA, USA, 2016; pp. 53–157.
4. Gondji, D.S.; Mohamadou, L.L.; Shouop, C.J.G.; Ateba, J.F.B.; Saïdou. Assessment of trace elements pollution and their potential health risks in the cobalt–nickel bearing areas of Lomié, East Cameroon. *Environ. Monit. Assess.* **2022**, *194*, 127. [CrossRef]
5. Omotehinse, A.O.; Ako, B.D. The environmental implications of the exploration and exploitation of solid minerals in Nigeria with a special focus on Tin in Jos and Coal in Enugu. *J. Sustain. Min.* **2019**, *18*, 18–24. [CrossRef]
6. Mensah, A.K.; Mahiri, I.O.; Owusu, O.; Mireku, O.D.; Wireko, I.; Kissi, E.A. Environmental Impacts of Mining: A Study of Mining Communities in Ghana. *Appl. Ecol. Environ. Sci.* **2015**, *3*, 81–94. [CrossRef]
7. Mbewe, H. Stakeholder Influence in Promoting Environmental Sustainability in the Mining Industry. Ph.D. Thesis, Walden University, Minneapolis, MN, USA, 2017. Available online: https://scholarworks.waldenu.edu/dissertations/3620/#:~{}:text=Stakeholder%20Influence%20in%20Promoting%20Environmental%20Sustainability%20in%20the,framework%20for%20mining%20industry%20operations%20have%20been%20inconsistent (accessed on 25 May 2021).
8. Ayoo, B.A. *Assessment of Occupational Safety Compliance in Small-Scale Gold Mines in Siaya County*; University of Nairobi: Nairobi, Kenya, 2018; Available online: https://scholar.google.com/scholar (accessed on 25 May 2021).
9. United Nations. *United Nations Scientific Committee on the Effect of Atomic Radiation, Sources and Effects of Ionizing Radiation*; UNSCEAR Report 2000; United Nations: New York, NY, USA, 2000.
10. Pereira, R.; Barbosa, S.; Carvalho, F.P. Uranium mining in Portugal: A review of the environmental legacies of the largest mines and environmental and human health impacts. *Environ. Geochem. Health* **2014**, *36*, 285–301. [CrossRef]
11. Minter, K.M.; Jannik, G.T.; Hinck, J.E.; Cleveland, D.; Kubilius, W.P.; Kuhne, W.W. Biota dose assessment of small rodents sampled near breccia pipe uranium mines in the grand canyon watershed. *Health Phys.* **2019**, *117*, 20–27. [CrossRef]
12. Wong, M.H. Ecological restoration of mine degraded soils, with emphasis on metal contaminated soils. *Chemosphere* **2003**, *50*, 775–780. [CrossRef]
13. Singh, A.; Prasad, S.M. Remediation of heavy metal contaminated ecosystem: An overview on technology advancement. *Int. J. Environ. Sci. Technol.* **2015**, *12*, 353–366. [CrossRef]
14. Deng, H.; Ye, Z.H.; Wong, M.H. Accumulation of lead, zinc, copper and cadmium by 12 wetland plant species thriving in metal-contaminated sites in China. *Environ. Pollut.* **2004**, *132*, 29–40. [CrossRef]
15. Dhir, B.; Sharmila, P.; Saradhi, P.P. Potential of Aquatic Macrophytes for Removing Contaminants from the Environment. *Crit. Rev. Environ. Sci. Technol.* **2009**, *39*, 754–781. [CrossRef]
16. Younger, P.L. Environmental impacts of coal mining and associated wastes: A geochemical perspective. *Geol. Soc. Lond. Spec. Publ.* **2004**, *236*, 169–209. [CrossRef]
17. Holden, W.N. Mining amid typhoons: Large-scale mining and typhoon vulnerability in the Philippines. *Extr. Ind. Soc.* **2015**, *2*, 445–461. [CrossRef]
18. Sahu, H.; Dash, E. Land Degradation due to Mining in India and its Mitigation Measures. *Proc. Second Int. Conf. Environ. Sci. Technol. Febr.* **2011**, *6*, 26–28. Available online: http://dspace.nitrkl.ac.in/dspace/handle/2080/1411%0Ahttp://www.ipcbee.com/vol6/no1/29-F00045.pdf (accessed on 23 July 2021).
19. Jang, J.; Kim, T.-M.; Cho, C.-H.; Lee, D.S. Radiological Safety Assessment for a Near-Surface Disposal Facility Using RESRAD-ONSITE Code. *J. Nucl. Fuel Cycle Waste Technol. JNFCWT* **2021**, *19*, 123–132. [CrossRef]
20. Tawfik, A.A.; Ahmed, E.M. Radiological doses and risk assessment of NORM scrap metal by using RESRAD-RECYCLE computer code. *Open J. Model. Simul.* **2014**, *2014*, 34–42. [CrossRef]

21. Yu, C.; Zielen, A.J.; Cheng, J.-J.; LePoire, D.J.; Gnanapragasam, E.; Wallo III, A.; Williams, W.A.; Peterson, H. *User's Manual for RESRAD Version 6*; ANL/EAD-4; Argonne National Laboratory, Environmental Assessment Division: Argonne, IL, USA, 2001.
22. Vukašinović, I.; Todorović, D.; Đorđević, A.; Rajković, M.B.; Pavlović, V.B. Depth Distribution of 137Cs in Anthrosol from the Experimental Field 'Radmilovac' Near Belgrade, Serbia. *Arch. Ind. Hyg. Toxicol.* **2018**, *64*, 425–430. [CrossRef] [PubMed]
23. Djelic, G.; Krstic, D.; Stajic, J.M.; Milenkovic, B.; Topuzovic, M.; Nikezic, D.; Vucic, D.; Zeremski, T.; Stankovic, M.; Kostic, D. Transfer factors of natural radionuclides and 137 Cs from soil to plants used in traditional medicine in central Serbia. *J. Environ. Radioact.* **2016**, *158*, 81–88. [CrossRef]
24. BUCREP. Planning de Publication des Résultats du 3ème RGPH. 2021. Available online: http://www.bucrep.cm/index.php/fr/recensements/3eme-rgph/20-3eme-rgph/presentation (accessed on 23 July 2021).
25. Le Planificateur. Météo Et Climat A Abong Mbang Au Cameroun. 2021. Available online: https://planificateur.a-contresens.net/afrique/cameroun/est/abong_mbang/2236053.html (accessed on 23 July 2021).
26. Yongue-Fouateu, R.; Ghogomu, R.T.; Penaye, J.; Ekodeck, G.E.; Stendal, H.; Colind, F. Nickel and cobalt distribution in the laterites of the Lomie region, south-east Cameroon. *J. Afr. Earth Sci.* **2006**, *45*, 33–47. [CrossRef]
27. Bobbo, M.O.; Ndjana, J.E.N., II; Suzuki, T.; Kudo, H.; Hosoda, M.; Owono, L.C.O.; Tokonami, S. Occupational Natural Radiation Exposure at the Uranium Deposit of Kitongo, Cameroon. *Radioisotopes* **2019**, *68*, 621–630. [CrossRef]
28. Davidgarlandjones. Chèvre du Cameroun: Caractéristiques d'Entretien Et De Soins. 2021. Available online: https://davidgarlandjones.com/fr/biznes/5746-kamerunskaya-koza-osobennosti-soderzhaniya-i-uhoda.html (accessed on 23 July 2021).
29. Higley, K.A.; Domotor, S.L.; Antonio, E.J. A kinetic-allometric approach to predicting tissue radionuclide concentrations for biota. *J. Environ. Radioact.* **2003**, *66*, 61–74. [CrossRef]
30. Sotiropoulou, M.; Florou, H. Radiological risk assessment in the terrestrial ecosystem: Comparative study of two software tools used for dose rate calculations. Environ. *Sci. Pollut. Res.* **2020**, *27*, 18488–18497. [CrossRef] [PubMed]
31. DOE. *DOE-STD-1153-2019: A Graded Approach for Evaluating Radiation Doses to Aquatic and Terrestrial Biota*; Final Technical Standard; U.S. Department Energy: Washington, DC, USA, 2002.
32. Higley, K.A.; Domotor, S.L.; Antonio, E.J.; Kocher, D.C. Derivation of a screening methodology for evaluating radiation dose to aquatic and terrestrial biota. *J. Environ. Radioact.* **2003**, *66*, 41–59. [CrossRef]
33. Yu, C.; LePoire, D.J.; Gnanapragasam, E.; Arnish, J.; Kamboj, S.; Biwer, B.M.; Chen, J.J.; Chen, S.Y. Development of Probabilistic RESRAD 6.0 and RESRAD-BUILD 3.0 Computer Codes NUREG/CR-6697. ANL/EAD/TM-98 (Argonne: Argonne National Laboratory). Available online: http://resrad.evs.anl.gov/docs/NUREG_6697.pdf (accessed on 25 July 2021).
34. Tchuente, S.F.Y.; Bongue, D.; Kwato, G.N.M. NORM Measurements and Radiological Hazard Assessment in the Gold Mining Areas of Eastern Cameroon. *Radiat. Environ. Med.* **2017**, *6*, 22–28.
35. Onjia, A.; Dragovic, S.; Academy, M.M. Assessment of gamma dose rates from terrestrial exposure in Serbia and Montenegro. *Radiat. Prot. Dosim.* **2006**, *121*, 297–302. [CrossRef]
36. Njinga, R.L.; Tshivhase, V.M. Use of RESRAD-Onsite 7. 2 Code to Assess Environmental Risk around Tudor Shaft Mine Tailing Sites. *Environ. Nat. Resour. Res.* **2018**, *8*, 138–147. [CrossRef]
37. Ziajahromi, S.; Khanizadeh, M.; Nejadkoorki, F. Using the RESRAD Code to Assess Human Exposure Risk to ^{226}Ra, ^{232}Th, and ^{40}K in Soil. *Hum. Ecol. Risk Assess.* **2015**, *21*, 250–264. [CrossRef]
38. Ndjana, N.J.E., II; Engola, L.N.; Saïdou; Hosoda, M.; Bongue, D.; Suzuki, T.; Kudo, H.; Kwato, N.M.G.; Tokonami, S. Simultaneous Indoor Radon, Thoron and Thoron Progeny Measurements in Betare-Oya Gold Mining Areas, Eastern Cameroon. *Radiat. Prot. Dosim.* **2019**, *185*, 391–401. [CrossRef]
39. Saïdou; Tokonami, S.; Hosoda, M.; Ndjana, N.J.E., II; Takoukam, S.D.S. Naturel radiation exposure to the public in mining and ore bearing regions of Cameroon. *Radiat. Prot. Dosim.* **2019**, *184*, 391–396. [CrossRef]